Available online at www.sciencedirect.com

ScienceDirect

IFAC Papers Online CONFERENCE PAPER ARCHIVE

IFAC PapersOnLine 52-6 (2019) 19–24

Nonlinear Model Predictive Control to Reduce Network-Wide Traffic Emission

Deepak Ingole, Guilhem Mariotte, Ludovic Leclercq

University of Lyon, IFSTTAR, ENTPE
F-69518 Lyon, France
(e-mail:{deepak.ingole, guilhem.mariotte, ludovic.leclercq}@ifsttar.fr)

Abstract: In this paper, we propose a model-based perimeter gating control approach to improve network-wide emissions in an urban traffic network. An accumulation-based Macroscopic Fundamental Diagram (MFD) model of a single reservoir city is developed to describe the evaluation of traffic flows in a network. Moreover, a path flow distribution scheme using Dynamic User Equilibrium (DUE) discipline is designed to reproduce driver's adaptation to controlled flow. Perimeter gating control scheme using the Nonlinear Model Predictive Controller (NMPC) is developed to track the optimal green routing coefficient which will indirectly track the network-wide emission levels by manipulating the traffic flows into a reservoir. Simulation results show the effectiveness of the proposed scheme in improving the traffic emissions inside and outside the perimeter. Comparative analysis of nocontrol and NMPC shows that the proposed NMPC-based network-wide emission control strategy outperforms.

© 2019, IFAC (International Federation of Automatic Control) Hosting by Elsevier Ltd. All rights reserved.

Keywords: MFD, user equilibrium, optimal green routing, emissions, gating control, nonlinear MPC.

1. INTRODUCTION

Emissions generated by vehicles in urban traffic areas, especially when traffic becomes congested and vehicles start to idle in long queues, significantly increase the level of harmful gases in the air such as Carbon Monoxide (CO) and Dioxide (CO_2), Hydrocarbon (HC), Nitrogen Oxides (NO_x), *etc.* (Choudhary and Gokhale, 2016; Mascia et al., 2017). On the top of emissions, traffic congestion leads to increased fuel consumption and its cost on the societies. Vehicles are the dominant source of many air pollutant emissions in cities and congestion have the potential to significantly worsen ambient air quality, particularly near major highways. To deal with the problem of congestion and emissions in the urban traffic network, the application of control systems engineering has gained significant attention to ensure efficient and reliable operation of urban traffic networks. In recent years, significant efforts have been made to reduce the congestion by considering different control measures (such as traffic signal, ramp metering, speed control, route guidance, *etc.*) and perimeter control strategies (such as Proportional-Integral-Derivative (PID), Model Predictive Control (MPC), optimal control *etc.*,)

Most of the work in perimeter control domain considered the concept of Macroscopic Fundamental Diagram (MFD) to model the traffic dynamics in the urban networks. This concept provides a well-defined relation between space-mean flow and density (or vehicle accumulation). The idea of behind the MFD was proposed by Godfrey (1969) and similar approaches were introduced later by Daganzo (2007); Geroliminis and Daganzo (2008).

Macroscopic emission models are the conventional method to estimate network-wide emission rates. The emission at large scale so they only need average speed and travel distance as inputs. Some models in this category are: Mobile Source Emission Model (MOBILE) (EPA, 2003), Emission Factors (EMFAC) model (CARB, 2017) and COPERT V model (Ntziachristos et al., 2009), Handbook Emission Factors for Road Transport (HBEFA) (Keller, 2017), *etc.*

There is a trivial solution to minimize emission: no vehicle should travel in the network. Optimal routing is certainly a more suitable solution as moving some vehicles from short path with high-level congestion to a longer one with higher speed can reduce emission. The optimal strategy should balance speed and distance as long paths may be counter prohibitive. However, optimal strategy will have some operational loss as it requires that people follow optimal guidance which means that some have to take longer routes should experience higher travel times. This paper investigates the inherent control strategy trying to achieve optimal routing by controlling the flow at the different city gates. Selfish user discipline (Dynamic User Equilibrium (DUE)) will force some users to take urban freeways and go around the city center. Users will not require route guidance but the gating strategy will modify the travel time when crossing the city center and then modify the splitting coefficient between the city center and urban freeways for all (Origin Destination) OD pairs. In short, our network-wide emission control scheme is composed of two layers. The first layer (optimal green routing) determines for the next time horizon the optimal splitting coefficient for all OD pairs (only two alternatives are possible for each OD). The second layer is a Nonlinear Model Predictive Control (NMPC)-based gating controller, which determine the flow limits that can enter the city at each time-step over the time horizon

2405-8963 © 2019, IFAC (International Federation of Automatic Control) Hosting by Elsevier Ltd. All rights reserved.
Peer review under responsibility of International Federation of Automatic Control.
10.1016/j.ifacol.2019.08.142

in order to DUE discipline distribute users among both alternative to be as close as possible to the optimal splitting coefficient. The efficiency of the proposed scheme is demonstrated through a case study of a single reservoir city and its performance is analyzed and compared with the nocontrol case.

2. NETWORK MODELING

2.1 The Network

The city network under consideration comprised of a homogeneous urban reservoir with one internal regional route and six transferring regional routes. Each transferring route has a freeway alternative (thus six freeways outside the reservoir in total), as depicted in Fig. 1. In this study, a regional route, or simply "route" in the following, corresponds to the aggregation of multiple individual paths on the real city street network that shares some characteristics in common (*e.g.* similar topology or length, following the same sequence of reservoirs in multi-reservoir systems, *etc*). All six transferring routes also include an inbound link (IL) at the reservoir entry.

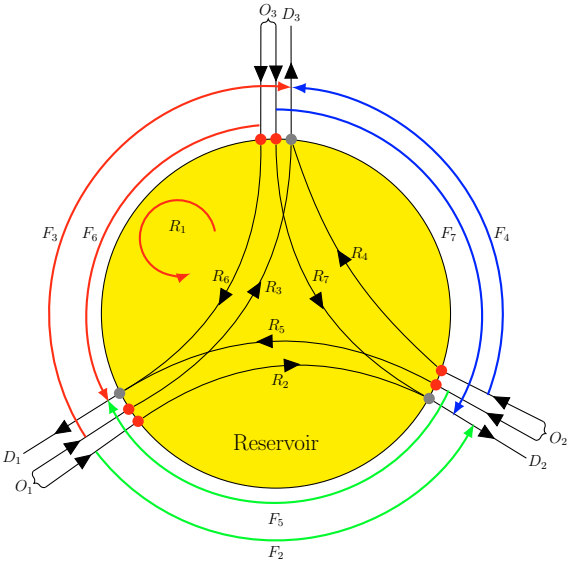

Fig. 1. Single reservoir network with one internal route (R_1), six external routes ($R_2, \ldots, R_7$), six freeways ($F_2(t), \ldots, F_7(t)$), and six inflow controlled gates.

We assume that the traffic dynamics of the reservoir is described by a well-defined production-MFD $P(n)$ (in [veh·m/s]), or equivalently, a speed-MFD $V(n)$ (in [m/s]), where n (in [veh]) is the total number of circulating vehicles in the reservoir. The production-MFD is notably defined by the following characteristic values: jam accumulation n_j, critical accumulation n_c, maximum production or capacity $P_c = P(n_c)$, and free-flow speed $\tilde{v} = dP(0)/dn$. Each inbound link is described by a point-queue model, and each freeway is described by a conservation equation with a fixed delay (assumed to be always in free-flow conditions with a constant mean speed).

2.2 MFD Traffic Model

In this section, we introduce the accumulation-based MFD model of the reservoir (see the foundations in Daganzo, 2007; Geroliminis and Daganzo, 2008), which represents the aggregated dynamics of the city network. The accumulation-based model with $\mathcal{R}$ regional routes of different lengths L_i has been proposed in Geroliminis (2015) and further extended in Mariotte and Leclercq (2018). The accumulations n_i are the numbers of vehicles traveling on each route R_i inside the reservoir, satisfying the following system (Geroliminis, 2015):

$$\frac{dn_i}{dt} = q_{\text{in},i}(t) - q_{\text{out},i}(t), \qquad \forall i \in \{1, \ldots, \mathcal{R}\}, \tag{1}$$

where $q_{\text{in},i}(t)$ and $q_{\text{out},i}(t)$ are respectively the effective inflow and outflow for route i.

In this work, we use the model of flow exchange at perimeter proposed by Mariotte and Leclercq (2018) to define $q_{\text{in},i}(t)$ and $q_{\text{out},i}(t)$. The effective inflow $q_{\text{in},i}(t)$ for a transferring route R_i is the result of the competition between a corresponding demand $\lambda_i(t)$ from the inbound link, an entry supply function $I_i(n_i, n)$ that mimic the congestion in the reservoir reaching the entry, and a gating inflow $u_i^\star(t)$ given by the NMPC controller. We also account for a queue at the entry of each route (described by a point-queue model) to store the waiting vehicles when the demand is not satisfied. These vehicles are physically waiting on the corresponding inbound link in our network. The inflow of the internal route is assumed to be unrestricted, thus equal to its demand:

$$q_{\text{in},i}(t) = \begin{cases} \min(\lambda_i(t), I_i(n_i(t), n(t)), u_i^\star(t)), & \forall i \geq 2, \\ \lambda_i(t), & i = 1. \end{cases} \tag{2}$$

For the transferring routes, the shape of the entry supply functions is still discussed in the literature. Here we adopt the model proposed in Mariotte and Leclercq (2018) with a scaling factor $\alpha > 1$ to ensure that these functions are not too restrictive:

$$I_i(n_i, n) = \begin{cases} \frac{n_i}{n}\frac{\alpha P_c}{L_i}, & \text{if } n < n_c, \\ \frac{n_i}{n}\frac{\alpha P(n)}{L_i}, & \text{otherwise.} \end{cases} \tag{3}$$

The effective outflow $q_{\text{out},i}(t)$ for a transferring route R_i is the result of the competition between its corresponding demand function $O_i(n_i, n)$ representing the reservoir dynamics, and an eventual exogenous limitation $\mu_i(t)$ representing some bottleneck at the exit of the route. As in Mariotte and Leclercq (2018), we assume the demand function to be maximum in over-saturated conditions for the transferring routes. This assumption is aimed at reproducing the effect of queuing vehicles at the reservoir exit when a bottleneck $\mu_i(t)$ effectively restricts the outflow. For the internal route, the outflow is supposed unrestricted and described by a decreasing function $O_i(n_i, n)$ to mimic internal congestion. We have thus:

$$\forall i \geq 2, \qquad O_i(n_i, n) = \begin{cases} \frac{n_i}{n}\frac{P(n)}{L_i}, & \text{if } n < n_c, \\ \frac{n_i}{n}\frac{P_c}{L_i}, & \text{otherwise.} \end{cases} \tag{4}$$

$$i = 1, \qquad O_i(n_i, n) = \frac{n_i}{n}\frac{P(n)}{L_i}. \tag{5}$$

Then, the effective outflows $q_{\text{out},i}(t)$ for both internal and transferring routes are calculated with the following relationships (Mariotte and Leclercq, 2018):

$$q_{\text{out},k}(t) = \min(\mu_k(t), O_k(n_k, n)), \tag{6}$$

where $k = \arg\min_{1 \leq i \leq N} \frac{\mu_i}{O_i(n_i, n)}$ and

$$q_{\text{out},i}(t) = \frac{n_i(t)}{n_k(t)} \frac{L_k}{L_i} q_{\text{out},k}(t), \qquad \forall i \neq k. \tag{7}$$

These relationships ensure the inter-dependency between outflows through the reservoir MFD $P(n)$ or $V(n)$, when the formulation of (4) is used. For more details about the considered accumulation-based model see Mariotte et al. (2017); Mariotte and Leclercq (2018).

3. ROUTING DISCIPLINE AND EMISSION CALCULATIONS

3.1 User Equilibrium Discipline

As shown in Fig. 1, the users willing to enter route R_i ($i \geq 2$) can choose to take the freeway F_i instead of entering the inbound link and crossing the reservoir to reach their destination. The freeway F_i is assumed to have a much higher capacity than all the city street represented by route R_i, so that its traffic conditions are always free-flow. Hence, if we assume that these travelers are making their choices according to DUE, we should have the following relationships in travel time at any time t:

$$\begin{cases} T_{IL,i}(t) + T_{R,i}(t + T_{IL,i}(t)) < T_{F,i} \Leftrightarrow \begin{array}{l}\text{no one}\\ \text{chooses}\\ \text{the freeway,}\end{array} \\ T_{IL,i}(t) + T_{R,i}(t + T_{IL,i}(t)) = T_{F,i} \Leftrightarrow \begin{array}{l}\text{at least one}\\ \text{user chooses}\\ \text{the freeway,}\end{array} \end{cases} \tag{8}$$

where $T_{F,i}$ is the freeway free-flow travel time, $T_{IL,i}(t)$ and $T_{R,i}(t)$ are the exact predictive travel times on the inbound link and in the reservoir, respectively, for route R_i (that will be experienced by users entering the reservoir or the inbound link at t). The inbound link is assumed to have a total length $L_{IL,i}$, and to consist of two parts: the first one is free-flow with speed $\tilde{v}_{IL,i}$, and the second one is congested, dynamically represented by a point-queue model. Thus its travel time consists of two terms: $T_{IL,i}(t) = L_{IL,i}/\tilde{v}_{IL,i} + \delta_{IL,i}(t + L_{IL,i}/\tilde{v}_{IL,i})$, where $\delta_{IL,i}(t)$ is the exact predictive delay in the inbound link (that will be experienced by users willing to enter the reservoir at t).

Both $\delta_{IL,i}(t)$ and $T_{R,i}(t)$ are the result of traffic dynamics that will be observed inside the reservoir after t. During the simulation, because we do not know the future evolution of the system at t, we choose to estimate these values based on the current state observation:

$$T^*_{R,i}(t) = L_i/V(n(t)), \tag{9}$$

$$\delta^*_{IL,i}(t) = n_{IL,i}(t)/q_{\text{in},IL,i}(t - dt), \tag{10}$$

where $n_{IL,i}(t)$ is the accumulation and $q_{\text{in},IL,i}(t-dt)$ is the effective inflow into the inbound link i, estimated from the previous time step $t - dt$ as we do not know it at t. Then, the estimation $T^*_{IL,i}(t)$ of the inbound link predictive travel time is directly obtained with $\delta^*_{IL,i}(t)$.

For a given route i, switching the users to the freeway F_i is achieved by splitting the inflow demand $\lambda_i(t)$ into the inbound link inflow $q_{\text{in},IL,i}(t)$ and the freeway inflow $q_{\text{in},F,i}(t)$ according to the following scheme:

Case 1 If $T^*_{IL,i}(t) + T^*_{R,i}(t) < T_{F,i}$, users switch to the reservoir route:

$$\gamma_i(t) = b_i.q_{\text{in},F,i}(t - dt)/\lambda_i(t - dt), \tag{11a}$$

$$q_{\text{in},IL,i}(t) = (1 - \gamma_i(t))\lambda_i(t), \tag{11b}$$

$$q_{\text{in},F,i}(t) = \gamma_i(t)\lambda_i(t). \tag{11c}$$

Case 2 Otherwise, users switch to the freeway:

$$\gamma_i(t) = b_i.q_{\text{in},F,i}(t - dt)/\lambda_i(t - dt) + b_i, \tag{12a}$$

$$q_{\text{in},IL,i}(t) = \max\left((1 - \gamma_i(t))\lambda_i(t); q^{\min}_{\text{in},IL,i}\right), \tag{12b}$$

$$q_{\text{in},F,i}(t) = \lambda_i(t) - q_{\text{in},IL,i}(t). \tag{12c}$$

The inflow splitting coefficient $\gamma_i(t) \in [0, 1]$ corresponds to the proportion of users on path i who just took the freeway alternative F_i to reach their destination. The calculation of this coefficient is smoothed via (11a) and (12a), which represents the progressive adaptation of the users to the instantaneous modification of the estimated travel times. The smoothing coefficients b_i are in [0,1]: the application of the UE discipline is quite instantaneous when the b_i are chosen close to 1.

Then, the accumulation in each inbound link i is governed by the following conservation equation:

$$\frac{dn_{IL,i}}{dt} = q_{\text{in},IL,i}(t) - q_{\text{out},IL,i}(t), \tag{13}$$

where the outflow is equal to the inflow in route i, i.e., $q_{\text{out},IL,i}(t) = q_{\text{in},i}(t)$. On the other hand, traffic dynamics in the freeway is considered to be always in free-flow condition, thus represented by the following conservation equation with a fixed delay (the freeway free-flow travel time $T_{F,i}$):

$$\frac{dn_{F,i}}{dt} = q_{\text{in},F,i}(t) - q_{\text{in},F,i}(t - T_{F,i}). \tag{14}$$

3.2 Emission Model

We use emission macroscopic rules that provide the emission rate (in [g/km]) of a reference vehicle depending on the mean speed $v^*(t)$. These rules come from the COPERT IV framework (Ntziachristos et al., 2009) and has been integrated with the fourth-degree polynomial for simplicity Lejri et al. (2018). In this work, we obtained the Emission Factor (EF) model of (NO_x) and (CO_2) based on the reference emission data recorded for mean speed (v^*) profile of personal cars. Then, the evolution of emission level $E_{dt}(t)$ (in [g]) of one pollutant between t and $t + dt$ is calculated as:

$$E_{dt}(t) = EF(v^*(t)) \cdot n^*(t) \cdot v^*(t) \cdot dt, \tag{15}$$

where $EF(v^*(t))$ is the emission factor of the pollutant considered (in [g/km]), $n^*(t)$ the accumulation and $v^*(t)$ the mean speed at t. The emission factor $EF(v^*)$ is estimated through curve fitting technique applied to emission curves shown in Fig. 2 (a). $E_{dt}(t)$ corresponds to instantaneous emissions, because it is calculated for a small time step $dt = 1$ s. On route i in the reservoir, $n^*(t)$ is the partial accumulation $n_i(t)$, and $v^*(t)$ is the reservoir mean speed $v(t)$. In the IL for route i, $n^*(t)$ is the link accumulation $n_{IL,i}(t)$, and $v^*(t)$ is the link mean speed $v_{IL,i}(t)$. On the freeway, $n^*(t)$ is the freeway accumulation $n_f(t)$, and $v^*(t)$ is the freeway free-flow speed $\tilde{v}_f$. The mean speed on inbound link i is obtained as:

$$v_{IL,i}(t) = \frac{L_{IL,i}}{T_{IL,i}(t)}, \tag{16}$$

where $L_{IL,i}$ and $T_{IL,i}$ are respectively the inbound link length and travel time.

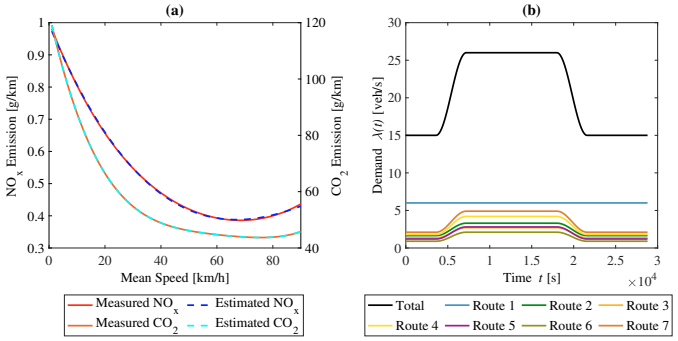

Fig. 2. Emission factors curves of NO_x and CO_2 (left column) and demand profiles used in the case study (right column).

3.3 Optimal Green Routing

As explained in the introduction, it is difficult to enforce optimal green route guidance when users are free to choose their route and often favor the shortest path in time. So, users usually comply to DUE discipline as discussed in Section 3.1. The routing is going to modify the proportion of travel time as both alternatives to match distribution close to the optimal splitting coefficient ($\beta_i^r(t) \in [0,1]$) for the all OD pairs. First, we have to determine those vehicles by assuming $\beta_i^r(t) = 1$ for the freeway and $(1-\beta_i^r(t))$ for the inbound link and reservoir routes. For this, we solve the Linear Programming (LP) problem to estimate optimal $\beta_i^r(t)$ that minimizes the total emission (E_τ) for predefined time horizon of $\tau = 60$ s. To calculate emission at each τ, we assume the fixed accumulation and speed (equal to the values at t) for $[t, t+\tau]$. The predicted E_τ is calculated as follows:

$$E_{\tau,f} = EF(\tilde{v}_f(t)) \cdot \lambda_i(t) \cdot \tau \cdot L_f, \tag{17a}$$
$$E_{\tau,\text{res.}} = EF(v(t)) \cdot \lambda_i(t) \cdot \tau \cdot L_i, \tag{17b}$$
$$E_{\tau,IL} = EF(v_{IL,i}(t)) \cdot \lambda_i(t) \cdot \tau \cdot L_{IL,i}. \tag{17c}$$

Combining (17a)-(17c) and considering optimal splitting coefficient, we get total emission in the network as

$$E_\tau = E_{\tau,f}\beta_i^r(t) + (E_{\tau,\text{res.}} + E_{\tau,IL})(1-\beta_i^r(t)). \tag{18a}$$

To find the optimal splitting coefficient $\beta_i^r(t)$ an LP problem is formulated as:

$$\min_{\beta_i^r(t)} \; E_{\tau,f}\beta_i^r(t) + (E_{\tau,\text{res.}} + E_{\tau,IL})(1-\beta_i^r(t)), \tag{19a}$$
$$\text{s.t. } 0 \le \beta_i^r(t) \le 1, \quad \forall t \in [t, t+\tau]. \tag{19b}$$

After obtaining the β_i^r trajectory, it is smoothed by Method of Successive Averages (MSA) as follows:

$$\beta_i^r(t) = \frac{1}{3}\beta_i^r(t) + \frac{2}{3}\beta_i^r(t-dt). \tag{20}$$

The value of controlled variable $\beta_i(t)$ was measured at the exit of reservoir with the following expression:

$$\beta_i(t) = 1 - (q_{\text{out},i}(t-dt)/\lambda_i(t-dt)). \tag{21}$$

4. NONLINEAR MODEL PREDICTIVE CONTROL

Nonlinear MPC is a advanced control technique were in a given objective function is minimized by solving a Constrained Finite-Time Optimal Control (CFTOC) problem. NMPC as a CFTOC problem for reference (splitting coefficient $\beta_i^r(t)$) tracking is represented as follows:

$$\min_{u_0,\ldots,u_{N-1}} \sum_{k=0}^{N-1} \left(||y_k - y_{\text{ref},k})||_Q^2 + ||\Delta u_k||_R^2 \right), \tag{22a}$$

s.t.

$$x_{k+1} = f(x_k, u_k), \qquad \forall k \in \{0,\ldots,N-1\}, \tag{22b}$$
$$y_k = g(x_k, u_k), \qquad \forall k \in \{0,\ldots,N-1\}, \tag{22c}$$
$$\Delta u_k = u_k - u_{k-1}, \qquad \forall t \in \{0,\ldots,N-1\}, \tag{22d}$$
$$u_{\min} \le u_k \le u_{\max}, \qquad \forall t \in \{0,\ldots,N-1\}, \tag{22e}$$
$$u_{-1} = u(t-1), \tag{22f}$$
$$x_0 = x(t), \tag{22g}$$

where $x \in \mathbb{R}^{n_x}$, $y \in \mathbb{R}^{n_y}$, and $u \in \mathbb{R}^{n_u}$ are the vector of state, output, and input, respectively. In (22a), y_{ref} corresponds to the reference trajectory of splitting coefficients $\beta_i^r(t)$ and y corresponds to the outputs corresponding to splitting coefficient $\beta_i(t)$. The cost function is weighted by $Q \succeq 0$ and $R \succ 0$. The function f in (22b) describes the nonlinear dynamics of the traffic network under consideration which is as give by (1). The optimization is performed with respect to $u_0,\ldots,u_{N-1}$. Then, as per the concept of a receding horizon implementation,only the first optimized input, i.e., $u_0^\star$ is implemented to the system in (1) and the whole procedure is repeated at a subsequent time instant for a new value of the initial condition in (22g).

In the implementation, sample time of 1 s is considered to measure the traffic states (x_{k+1}) of the system whereas the optimal control actions ($u_0^\star$) and references $\beta_i^r(t)$ are updated at each 60 s. Prediction horizon (N_p), output penalty (Q), and input penalty (R) was set to 10, $0.001\times\mathbb{I}_{(n_u\times n_u)}$, and $100\times\mathbb{I}_{(n_y\times n_y)}$, respectively. The constrains on input flow rate was set to $0.1 \le u_k \le 6$ m/s.

5. SIMULATION RESULTS

In order to demonstrate the effectiveness of the designed NMPC and optimal routing scheme, a case study has been considered and the results are compared with the Nocontrol (NC) case. The values of MFD model parameters used in the case study are given in the Table 1. Fig. 2 (b) shows

Table 1. Model parameters used in the case study. All freeways and inbound links also have the same characteristics.

Parameter	Value	Unit
Reservoir trip lengths (L_i)	[5 6 7 5.5 8 7.5 8.5]$\times 10^3$	m
Reservoir maximum production (P_c)	150000	veh·m/s
Reservoir free-flow speed ($\tilde{v}$)	14	m/s
Reservoir jam accumulation (n_j)	60000	veh
Reservoir critical accumulation (n_c)	12000	veh
Freeway trip length (L_f)	22500	m
Freeway free-flow speed ($\tilde{v}_f$)	14	m/s
Freeway free-flow travel time (T_f)	1428	s
Inbound link free-flow speeds ($\tilde{v}_{IL,i}$)	19	m/s
Inbound link trip lengths ($L_{IL,i}$)	2500	m

the inflow demand profiles of all routes used in case study.

Fig. 3 shows the response of NMPC scheme while tracking $\beta_i^r(t)$ trajectories. For control case, during network loading

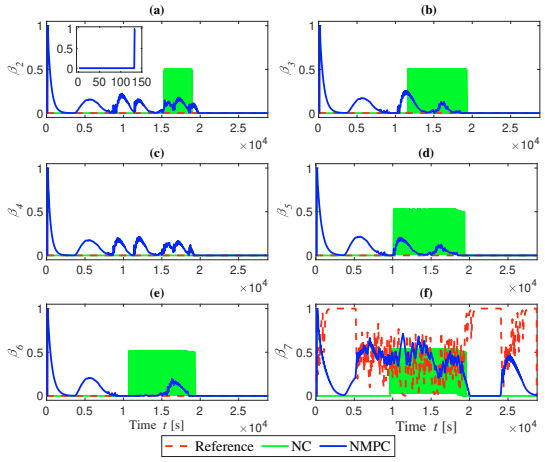

Fig. 3. Performance evaluation of splitting coefficients for nocontrol and NMPC.

period measured $\beta_i(t)$ values are zero as shown in zoom part of Fig. 3(a), during that time there was no outflow at the exit of reservoir. After that there was a gradual increase in the outflows and decrease in the $\beta_i(t)$ values. The spike in the $\beta_i(t)$ was due to the first outputs at the exit of reservoir. However, it can be observed that in some parts especially during high inflow demands (from 3600-18000 s),$\beta_1, \ldots, \beta_4$ values are not tracking their references. This is due to the DUE discipline which enforces the limitation on the number of users. For the NC case, $\beta_i(t)$ values are oscillating during high congestion, expect for the β_3 which is due to the highest outflow and low accumulation on the R_4. For β_6, reference values are oscillating between 0 and 1, which is because of the R_7 which have longest trip length.

Fig. 4 depicts the emission levels of NO_x and CO_2 and mean speed in the whole network (left column) and in the reservoir (right column). Note here that CO_2 is only monitored and has no contribution in the calculation of $\beta_i(t)$. It can be observe that with the NMPC scheme there is a significant decrees in the network-wide and reservoir emissions and increase in mean speeds. With NMPC, amount of NO_x is reduced by 329 kg and CO_2 by 22781 kg. It indicates that the proposed scheme is beneficial for perimeter area as well as in total.

Fig. 5 depicts the total emission levels of NO_x and CO_2 and mean speed on the inbound link (left column) and on the freeway (right column). With NMP, on the inbound links total (sum of IL_i) emissions are decreased and mean speed is increased. The oscillations in the mean speed are due to the inflow which is also oscillating (see Fig. 6(e)). As expected, with NMPC freeways have high emissions as compared to the NC. This is due to the fixed mean speed on all the freeways.

Fig. 6 presents the total accumulation, inflow, and outflow inside the reservoir (left column) and route wise accumulation, inflow, and outflow inside the reservoir (right column). It can be seen that during loading and unloading period the total accumulation inside the perimeter is almost similar in NC and NMPC case. Whereas during high demand period, NC drives reservoir in high congestion and NMPC keep accumulation around the critical value which is almost similar to tracking total accumulation

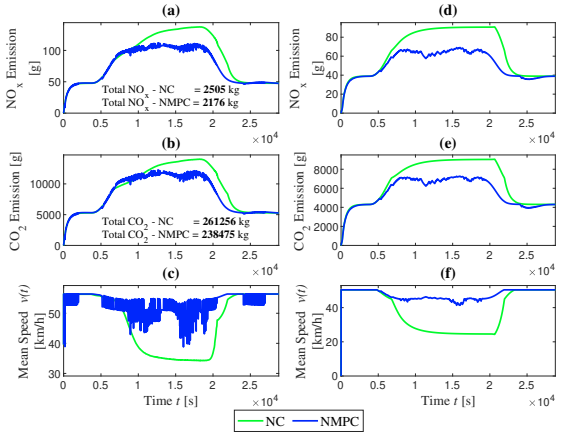

Fig. 4. Performance evaluations of network-wide emissions and mean speed (left column) and reservoir emission and mean speed (right column) for nocontrol and NMPC.

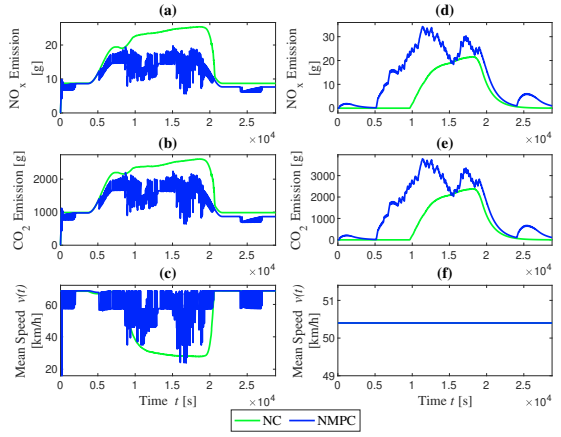

Fig. 5. Response of total emissions and mean speed on the inbound link (left column) and freeway (right column) for nocontrol and NMPC.

by controller. This is because of the improved inflow and outflow. The contribution of accumulation and flows in the total can be observed in right column of the Fig. 6.

Fig. 7 shows the accumulation on inbound link/queue (a) and accumulation on the freeways (b). It can be seen that for nocontrol case during high demand period all IL has long queues and with NMPC queues are decreased due to the increased mean speeds and increased inflow to the reservoir. In case of freeways, F_7 have more accumulation in both cases due to the trip length of R_7.

5.1 Comparative Analysis

In this section, the numerical analysis of above results is discussed. Table 2 gives the summary of performance evaluation of nocontrol and gating control schemes. Given values in the table are calculated for the whole simulation time (8 h) in the form of the percentage (%) with respect to the uncontrol case. The values indicated in red color shows a negative effect, and values in green color shows a significant positive effect of the NMPC scheme. Table 2 shows the four performance indicators about emission, Total Time Spent (TTS) and mean speed in the reservoir, inbound links, freeways, and whole network. The results

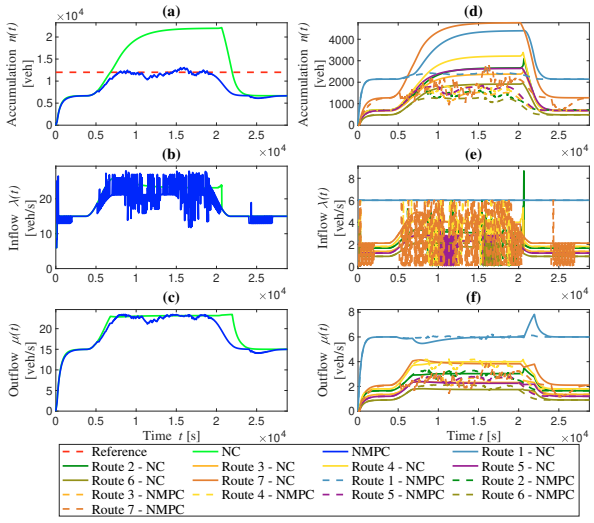

Fig. 6. Response of total (left column) and route wise (right column) accumulation, inflow, and outflow for nocontrol and NMPC.

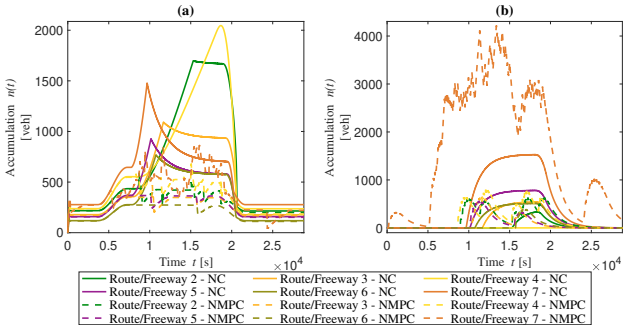

Fig. 7. Response of accumulation on the inbound links (a) and freeways (b) for nocontrol and NMPC.

Table 2. Performance comparison of nocontrol and NMPC gating control schemes.

Indicator	Reservoir	IL	Freeway	Total
Emission NO_x	-21.0	-25.50	109.7	-13.10
Emission CO_2	-16.85	-24.33	109.7	-8.72
TTS	-25.85	-30.50	-31.80	-25.0
Mean Speed	24.88	18.97	0	13.81

indicate that NMPC scheme with optimal green routing is capable of improving green mobility in the network, as it shows decreased values of emissions (expect on freeways), TTS and mean speed, in comparison to the NC case. As expected freeways have high emissions due to constant speed and long distance, but higher improvements in others parts compensates it which intern shows decrease in network-wide emission.

6. CONCLUSIONS

We have proposed an approach to reduce network-wide emissions by using optimal green routing and NMPC-based gating control strategies. NMPC strategy is developed based on an accumulation-based MFD model, along with that a DUE scheme is developed for the path distribution assuming the freeway option. Further, an optimal green routing scheme is proposed to find splitting coefficients which give the optimal route choice corresponding low emission route. Reference trajectories of the splitting coefficients are predicted and utilized in the NMPC scheme developed to track optimal splitting coefficients. The performance of the developed approach is demonstrated through a single reservoir urban network. Simulation results show the potential for significant improvement in network-wide emission, TTS, and mean speed. A further observation is that the proposed approach also helps to protect the reservoir from severe congestion.

ACKNOWLEDGEMENTS

The research leading to these results has received funding from the European Research Council (ERC) under the European Union's Horizon 2020 research and innovation program (grant agreement No 646592 – MAGnUM project).

REFERENCES

CARB (2017). *EMFAC 2017 User's Guide*.

Choudhary, A. and Gokhale, S. (2016). Urban real-world driving traffic emissions during interruption and congestion. *Transportation Research Part D: Transport and Environment*, 43, 59–70.

Daganzo, C.F. (2007). Urban gridlock: Macroscopic modeling and mitigation approaches. *Transportation Research Part B: Methodological*, 41(1), 49–62.

EPA, U. (2003). *User's guide to MOBILE6.1 and MOBILE6.2 Mobile Source Emission Factor Model*.

Geroliminis, N. (2015). Cruising-for-parking in congested cities with an MFD representation. *Economics of Transportation*, 4(3), 156–165.

Geroliminis, N. and Daganzo, C.F. (2008). Existence of urban-scale macroscopic fundamental diagrams: Some experimental findings. *Transportation Research Part B: Methodological*, 42(9), 759–770.

Godfrey, J. (1969). The mechanism of a road network. *Traffic Engineering & Control*, 8(8).

Keller, M. (2017). *Handbook of emission factors for road transport (HBEFA) 3.3*.

Lejri, D., Can, A., Schiper, N., and Leclercq, L. (2018). Accounting for traffic speed dynamics when calculating copert and phem pollutant emissions at the urban scale. *Transportation research part D: Transport and Environment*, 63, 588–603.

Mariotte, G. and Leclercq, L. (2018). MFD-based simulation: Spillbacks in multi-reservoir networks. *97th Annual Meeting TRB, Washington D.C.*

Mariotte, G., Leclercq, L., and Laval, J.A. (2017). Macroscopic urban dynamics: Analytical and numerical comparisons of existing models. *Transportation Research Part B: Methodological*, 101, 245–267.

Mascia, M., Hu, S., Han, K., North, R., Van Poppel, M., Theunis, J., Beckx, C., and Litzenberger, M. (2017). Impact of traffic management on black carbon emissions: a microsimulation study. *Networks and Spatial Economics*, 17(1), 269–291.

Ntziachristos, L., Gkatzoflias, D., Kouridis, C., and Samaras, Z. (2009). COPERT: a european road transport emission inventory model. In *Information technologies in environmental engineering*, 491–504. Springer.